

COMET BOWELL 1980b

MICHAEL F. A'HEARN^{a), b)} AND DAVID G. SCHLEICHER^{b)}
Astronomy Program, University of Maryland, College Park, Maryland 20742

PAUL D. FELDMAN^{a)}
Physics Department, Johns Hopkins University, Baltimore, Maryland 21218

ROBERT L. MILLIS AND DON T. THOMPSON

Lowell Observatory, Flagstaff, Arizona 86002
Received 29 September 1983; revised 28 December 1983

ABSTRACT

We have carried out optical filter photometry and optical and ultraviolet spectrophotometry of Comet Bowell over the period November 1980–June 1982. We have observed emission by OH at heliocentric distances to nearly 5 AU preperihelion with the OH emission implying a production rate which decreased, but with outbursts, as the comet approached perihelion. CN, however, did not appear until the comet was close to perihelion. The grains exhibited a larger back-scattering peak than has been observed in other comets and showed evidence for two populations and outbursts. The reflectivity of the grains was determined from 2600 Å to 2.2 μ and shows steep slopes in two regions, 3200–4000 Å and 1.2–1.6 μ , with shallower or negligible slopes in other regions. A self-consistent model is developed which explains the emission by OH at large distances as due to vaporization of H₂O from the grains which were already in the coma and from which the parent of CN had diffused. The subsequent emission near perihelion was due to vaporization of the nucleus itself. All observations are quantitatively consistent with a nucleus of radius several kilometers and a pre-existing halo of grains corresponding to a layer of a few meters if spread on the nucleus. We suggest that Comet Bowell is a useful prototype for the behavior of all dynamically new comets as they approach the Sun.

I. INTRODUCTION

The apparition of Comet Bowell 1980b presented a unique opportunity to study the solid particles in a dynamically new comet on its first approach to the Sun from the Oort cloud. Originally discovered at Lowell Observatory by E. Bowell on 13 March 1980 (Bowell 1980) when it appeared very close to Jupiter in the sky, the comet subsequently passed very close in space (0.23 AU) to Jupiter. The perturbations by Jupiter changed the orbit into the most strongly hyperbolic one on record, but a careful integration backwards by Everhart and Marsden (1983) showed that the original orbit was very weakly elliptical and thus that the comet was dynamically a new one from the Oort cloud and not an interstellar comet.

The comet already showed an extensive coma with a purely continuous spectrum (e.g., Cochran and McCall 1980) when it was first discovered at a heliocentric distance beyond 7 AU. This coma was modeled by Sekanina (1982) who concluded that the particles in the coma were not being produced at the time but rather were very large ones (≈ 0.5 mm) which either had been always in orbit about the nucleus or had been lifted from the surface by transient activity at very large distances from the Sun. The perihelion distance of Comet Bowell, 3.36 AU, permitted continued observation over several years at a very advantageous heliocentric distance, specifically the distance at which ordinary ice of H₂O should just begin to vaporize significantly. Thus it was possible to study the evolution of the particles with time in a way that is not possible for most new comets.

^{a)} Guest Investigator with the International Ultraviolet Explorer.

^{b)} Visiting Astronomer, Cerro Tololo Inter-American Observatory, which is operated by AURA under contract with the National Science Foundation.

II. OBSERVATIONS

a) Filter Photometry

Our program of filter photometry uses the same basic observational methods and reduction techniques that have been used on numerous previous comets (see, e.g., Millis *et al.* 1982, or A'Hearn 1982 for recent discussions). This technique is by far the most useful one for monitoring variations with time and for surveying numerous comets although the proper interpretation of the results often requires supplementary information from spectrophotometry and/or imaging techniques. We have, in fact, obtained supplementary spectrophotometric data for this program because the comet was such an unusual one that the interpretation of the photometric data might be questioned. The photometric program utilized many different telescopes and two different (but matched) sets of interference filters. Table I lists the observational circumstances and the deduced fluxes, both in the continuum and in discrete emission features. Because Comet Bowell crossed the Milky Way, there were frequently problems with background stars, particularly in 1982. We were always careful to stop observing whenever visible stars appeared in the field of view with the comet and we offset in various directions and by varying amounts in order to make sky measurements in regions that were clear of visible stars. A significant amount of observing time was lost due to the presence of these background stars in the field of view. On several occasions we monitored the brightness of star plus comet when the comet passed particularly close to a star but in no case were we able to detect any dimming (at $\lesssim 5\%$ precision) which might be attributed to attenuation of the starlight by the cometary grains.

In order to compare measurements taken at different times, under differing geometrical circumstances, and with

TABLE I. Photometric observations.

UT Date	r [AU]	Δ [AU]	Phase	Telescope ¹	Diaphragm ²		$\log F$ [erg cm ⁻² s ⁻¹] ³				$\log F_{\lambda}$ [erg cm ⁻² s ⁻¹ Å ⁻¹] ³								
					[arcsec]	ρ [10 ⁴ km]	OH A-X, $\Delta v=0$	GN B-X, $\Delta v=0$	C ₃ ($\lambda 4050$)	C ₂ d-a, $\Delta v=0$	$\lambda 3300$	$\lambda 3675$	$\lambda 5240$						
1980																			
Nov 14.52	5.554	6.116	8 ²⁰	L72	19'6	4.35	-	<-13.7	-	-12.89 +14,-.23	-	-	14.47 ±.04						
1981																			
Jan 5.43	5.254	5.035	10 ²⁷	L72	28.0	5.11	-12.35 ±.06	<-13.45	-	<-11.5	-14.65 ±.03	-14.48 ±.02	-13.96 ±.20						
Mar 12.36	4.785	3.822	3 ²³	L72	19.6	2.72	<-12.04	<-13.01	<-12.04	<-12.14	-14.18 ±.14	-14.31 ±.12	-13.99 ±.01						
Apr 5.41	4.636	3.649	2 ²³	L72	38.7	5.12	-11.60 ±.13	<-12.92 ⁴	<-12.35	-12.04 ±.08	-13.95 ±.08	-13.89 ±.04	-13.60 ±.01						
Apr 6.39	4.630	3.646	2 ²⁶	L72	13.6	1.80	-12.37 ±.08	<-13.35 ⁴	<-13.0	-12.43 ±.10	-14.27 ±.02	-14.25 ±.02	-13.99 ±.02						
1982																			
Jan 30.53	3.387	3.834	14 ²⁰	L72	28.0	3.89	-12.42	-12.14	-12.43	-12.00	-13.99 ±.15	-	-13.65						
Mar 6.51	3.364	3.381	16 ²⁹	L42	37.5	4.60	<-11.86	-12.18 ±.09	-	-11.93 ±.08	-13.92 ±.06	-13.77 ±.06	-13.51 ±.01						
Mar 24.49	3.366	3.144	17 ²²	L42	37.5	4.27	-	-12.40 ±.18	-	-11.80 ±.19	-	-13.82 ±.03	-13.58 ±.04						
Mar 26 35	3.366	3.120	17 ²²	C24	49.8	5.63	<-11.71 ⁴	-11.94 ±.14	<-11.84	-11.64 ±.08	-13.87 ±.20	-13.73 ±.10	-13.43 ±.02						
Mar 27.32	3.367	3.107	17 ²¹	C24	24.7	2.78	<-11.91 ⁴	-12.47 +12,-.34	<-12.05	-12.09 ±.17	-14.65 ±.17	-13.97 ±.10	-13.69 ±.02						
Mar 28.33	3.367	3.094	17 ²¹	C24	17.9	2.01	<-11.79 ⁴	<-12.2	<-12.26	-12.23 ±.13	-14.21 ±.16	-14.14 ±.06	-13.84 ±.02						
Mar 29.37	3.368	3.081	17 ²¹	C24	98.6	11.02	-11.38 ±.07	-11.53 ±.02	-11.93 ±.13	-11.38 ±.06	-13.45 ±.04	-13.45 ±.03	-13.16 ±.02						
Apr 23.54	3.388	2.785	15 ²⁰	M24	39.5	3.99	-	-12.22	<-12.20	-12.03	-13.70	-	-13.40						
Apr 24.50	3.390	2.775	14 ²⁹	M24	49.6	4.99	-	-	-	-11.17	-	-	-13.14						
Apr 25.55	3.391	2.764	14 ²⁸	M24	39.5 25.1	3.92 2.52	- -	- -	- -	- -11.88	-13.90 -	- -	- -13.62						
Apr 28.49	3.394	2.735	14 ²³	M24	39.5	3.92	-	-	-	-	-	-	-13.38						
Apr 28.44	3.394	2.735	14 ²⁴	L72	28.0	2.78	-11.95 +16,-.24	-12.20 ±.05	<-12.53	-11.89 ±.07	-13.70 ±.01	-13.68 ±.02	-13.45 ±.01						
					9.6	0.95	-12.18 +14,-.24	-13.06 +22,-.58	-	<-12.10	<-14.40 -	<-14.80	-13.96 ±.15						
Apr 30.45	3.397	2.716	14 ²⁰	L72	2.2	0.22	<-13.22	-13.73 ±.20	-	<-12.99	-15.53 ±.15	-15.23 ±.08	-14.96 ±.05						
					9.6	0.94	-12.29 ±.04	-12.98 ±.10	<-13.11	-12.41 ±.07	-14.08 ±.04	-14.52 ±.05	-13.99 ±.01						
May 29.40	3.447	2.513	7 ²⁷	L72	19.6	1.78	-12.30	-12.46	-13.07	-11.92	-13.86	-13.81	-13.57						
May 30.39	3.449	2.509	7 ²⁴	L72	19.6	1.78	-12.40 ±.09	-12.54 ±.03	-12.53	-11.99 ±.07	-13.91 ±.01	-13.88 ±.01	-13.58 ±.01						
Jun 24.32	3.509	2.493	0 ²²	L72	19.6	1.77	-12.89 +19,-.35	-12.53 ±.04	<-12.81	-11.93 ±.05	-13.83 ±.01	-13.72 ±.01	-13.43 ±.01						

1. L = Lowell Observatory, C = CTIO, M = Mauna Kea Observatory, telescope aperture in inches

2. First column gives angular diameter; second column gives radius projected at comet.

3. Where upper limits are given, they represent 2σ . Where errors are given, they represent \pm one standard deviation of the photometric precision using repeated measurements on the comet and allowing for the precision of the standard stars and of the continuum subtraction under emission bands. No errors are given where the data are incomplete or where only one measurement was made since meaningful errors can not readily be determined in these cases.

4. Although these measurements are individually less than 2σ , the agreement with other measurements (other nights and/or apertures) is better than 2σ .

widely varying fields of view, we have reduced all of the continuum measurements to the quantity Afp (given in Table III), the product of albedo, filling factor of grains within our field of view, and the linear radius of the field of view at the comet. The filling factor, f , is just the total cross section of grains within the field of view, $N(\rho)\sigma$, divided by the area of the field of view, $\pi\rho^2$, where σ is the cross section of a single grain. In all our work, the albedo A is a function of wavelength, λ , and of scattering angle, θ , and is defined as the ratio of the total light reflected by the cometary particles to

the total light removed from the solar flux by the cometary particles. In other words the total luminosity from the comet is given by $AN\sigma F_{\odot}/r^2$, and the product Af can be determined directly from the observations as $Af = (\Delta r/\rho)^2 F_{\text{com}}/F_{\odot}$, where Δ and ρ are in kilometers (or centimeters) but r is in AU, and where F_{\odot} is the solar flux at 1 AU, while F_{com} is the observed cometary flux. Strictly speaking, the appropriate cross section of the particles, σ , is the extinction cross section but in the absence of information about the extinction efficiency we will sometimes associate

the extinction cross section with the geometrical cross section. Our definition of albedo is a factor 4 larger than the albedo, $A_p(\theta)$, defined by Hanner *et al.* (1981). We include the factor ρ in our parameter $A_f\rho$ because, on a simple radial-outflow model, the resultant quantity should be independent of the field of view [since $N(\rho) \propto \rho$]. For the solar flux, F_\odot , we have used the fluxes of Neckel and Labs (1981) averaged over the bandpasses of our filters. As we will show below, the values of $A_f\rho$ deduced from the filter photometry agree well with the values deduced from spectrophotometry and also are usually independent of the field of view.

The fluxes of emission bands given in Table I generally have much larger errors than do the continuum fluxes. This is because the continuum was so strong relative to the emission features that the resultant subtraction of a slightly uncertain continuum leads to a large percentage error in the flux of an emission band. Because the resultant fluxes are so sensitive to the method of continuum subtraction, it is appropriate to review this aspect of our reductions. We have used our filters to observe four of the seven stars identified by Hardorp (1982, and references therein) as having spectral energy distributions identical to that of the Sun (HD 28099, 29461, 30246, and 186427). The colors of these stars in our system agree with each other within $\pm 0^m.01$. We use the continuum filters at 3675 Å and 5240 Å to determine the color excess (reddening) of the cometary grains relative to the Sun (color excesses given in Table III). We then predict the magnitude that the cometary continuum should have, e.g., in the 3870 (CN) filter using the magnitude differences observed for the solar analogs (e.g., $m_{3870} - m_{5240}$) with an allowance for reddening assuming that it is linear with wavelength. Since the reddening is generally small, the assumption of linearity leads to very little error unless there is significant structure in the reflectivity as a function of wavelength. The difference between the observed cometary magnitude, e.g., at λ 3870, and that predicted on the basis of the continuum filters is then attributed to the emission feature. Further details are given by A'Hearn (1983).

The errors quoted for the emission-band fluxes in Table I include the uncertainties due to the measured uncertainties of the continuum fluxes but they do not include any uncertainty due to the assumption of linearity or due to the assumption that the colors of the stellar analogs correspond to the colors of the Sun. Virtually every measurement of an emission band flux for OH, CN, or C_2 led to a positive detection. In only two cases did we deduce a negative flux for these features (we frequently deduced a negative flux for the C_3 feature), whereas one would have expected a 50% rate of deducing negative fluxes if there were no emission bands present. On the other hand, many of these positive detections were not, by themselves, statistically significant and we have therefore given in Table I the 2σ upper limits whenever the deduced flux was less than this amount. It should be noted that the upper limits are more common for the smaller fields of view than for the larger. This is due in part to the fact that a large field of view provides a better signal-to-noise ratio in the raw data, but it is more importantly due to the fact that the continuum is more strongly concentrated toward the nuclear region than are the emission bands. Thus the larger apertures have a much better contrast between the emission bands and the continuum. This advantage can sometimes lead to detection of a feature that is not seen spectrophotometrically just because most spectrophotometers use such a small field of view that there is not sufficient contrast between the emission feature and the continuum. We ad-

dress below the confirmation of the detections of emission features by spectrophotometric techniques to show that they are not due to the assumptions inherent in filter photometry.

The fluxes in the emission bands have been reduced to abundances using the standard fluorescence efficiencies. These abundances have then been extrapolated to the total abundance in the entire coma using a Haser model, and finally production rates have been deduced by assuming arbitrarily that the lifetimes of the species in seconds are given by the scale lengths of the Haser model in kilometers. [See A'Hearn (1982) for all the relevant numerical parameters.] In many cases we have lumped together all of the data from a single observing run to deduce an average production rate. Wherever errors are given in Table II, they are the standard deviation of the mean based on the differences from night to night and/or from one field of view to another. As in Table I, we have quoted 2σ upper limits where appropriate.

Note that the color excess described above and given in Table III can be related directly to the average slope of the curve of reflectivity versus wavelength:

$$\text{slope} = \frac{r(\lambda_2) - r(\lambda_1)}{r(\lambda_2) + r(\lambda_1)} \frac{2}{\Delta\lambda} = \frac{\alpha - 1}{\alpha + 1} \frac{2}{\Delta\lambda}, \quad (1)$$

where $\alpha = 10^{0.4\text{CE}}$ and CE = color excess. Thus a typical color excess of $0^m.3$ corresponds to a reflectivity which increases by 18% (of its mean value) per 1000 Å.

b) Optical Spectrophotometry

Although our original goal was to obtain simultaneous spectrophotometry from 2000 Å to 5μ in order to study the grains in detail (as well as to confirm the photometric results), it was not possible to achieve sufficient signal to noise using a spectrophotometer in the infrared. We therefore obtained only broadband photometry in the infrared and these data have been published elsewhere (A'Hearn *et al.* 1983). Furthermore, it was not possible to obtain observing time with a spectrum scanner at Cerro Tololo simultaneous with the observing time for the ultraviolet and infrared. We therefore must use filter photometry to take into account time variations between the two sets of spectrophotometric data. Nevertheless, this procedure should be quite reliable as discussed below.

Optical spectrophotometry was obtained with the 1.5-m telescope at CTIO in the period 29 March–3 April 1982. Because none of the "fast" spectrophotometric systems have ultraviolet sensitivity, it was necessary to use the rather less efficient two-channel Harvard scanner to cover the desired spectral range. Rather than switch the comet back and forth between the two channels, we normally observed the comet in only one channel and used the early portion of the night, before the comet rose, to measure the relative sensitivity of the two channels using standard stars. This procedure did require, however, that we separately determine the dark current in each channel at regular intervals and also separately determine the spectral responsivity of the two channels. The wide spectral range desired for our program necessitated separate observations for each of several different portions of the spectrum. Wavelengths below 5000 Å were observed in first order while longer wavelengths were observed in second order. It was also necessary to use several combinations of order-separating filters which left us with no suitable combination for the region 4000–4500 Å. All observations were made with a 1.22-mm exit slot providing 20-Å resolution for a point source. Both entrance apertures used, for the comet

TABLE II. Gas production.

Date [UT]	r [AU]	$\log Q(\text{gas}) [\text{s}^{-1}]^1$			
		OH	CN	C ₃	C ₂
1980:					
Nov 14.5	5.55	-	<15.4	-	<26.20
1981:					
Jan 5.4	5.25	28.87	<25.30	-	<26.92
Mar 12.4	4.78	<29.3	<25.83	<25.67	<26.1
Apr 5-6	4.63	29.19 ±.02	23.38 ² ±.03	<15.3	<16.16
1982:					
Jan 30.5	3.39	28.21	25.99	(24.6)	(25.9)
Mar 6.5	3.36	28.53	25.79	-	(25.8)
Mar 24.5	3.37	-	25.57	-	(25.9)
Mar 26-29 (CTIO Phot)	3.37	28.13 ² ±.11	25.76 ±.01	24.3 ±.1	25.80 ±.02
Mar 29 - Apr 3 (CTIO Spectro)	3.37	28.04	25.82	-	25.56
Apr 23-28 (MKO)	3.39	-	(25.5)	-	26.0 ±.2
Apr 27.6 (IUE)	3.39	28.06	-	-	-
Apr 28.4 (LO)	3.39	28.78 ±.15	25.84 ±.01	(24.4)	25.97 ±.01
Apr 30.4	3.40	29.11	25.89	<24.55	26.2
May 22.2 (IUE)	3.43	27.87	-	-	-
May 28.2 (IUE)	3.44	27.78	-	-	-
May 29-30	3.45	28.47 ±.05	25.72 ±.04	<24.51	26.16 ±.05
Jun 24.3	3.51	27.93	25.67	<24.29	26.21

1. Assumes lifetimes [s] = scale lengths [km] of Haser model. Values in () are very uncertain.
2. Combines several detections of less than 2σ each where internal agreement is better than 2σ .
3. Where errors are quoted, they are deduced from the scatter among independent observations with different aperture sizes. They thus include all sources of error including errors in centering on the nucleus and deviations from a Haser model. The errors deduced from observed counting statistics, extinction uncertainties, and standard star uncertainties are generally, but not always, smaller than this. Upper limits are usually from nights of poor photometric quality.

and the sky, had a diameter of 39.7 arcsec which projected to a total spectral width of approximately 25 Å in the plane of the exit slot. The entrance apertures were separated by nearly 3 arcmin. Stars were observed with smaller entrance apertures. As with the filter photometry, it was sometimes necessary to cease observing the comet when it passed close to stars or when stars were in the "sky" aperture.

Extinction was determined every night using scans of HD 120086 and HD 149363, typically with four or more forward-reverse scan pairs on each covering airmasses between 1.1 and 2.0, the same range over which the comet was observed.

On the three nights which turned out to be photometric, the extinction coefficient was the same to within the errors and we therefore used the mean value for the three nights. Red leaks at the ultraviolet wavelengths (which were observed in second order such that first-order red light passed the spectrometer) were checked using bright stars of late-G type (i.e., as red as the comet which was the reddest object in our program) and found to be negligible. The flux calibration

was provided by several standard stars from our photometric program, primarily HD 120086 and η Hya. The solar spectrum was estimated from scans of 35 Leo and HD 76151. Although these stars are not exact analogs of the Sun (Hardorp 1982, and references therein), they are only slightly different from the Sun and they deviate from the Sun in opposite directions such that their average should mimic the Sun to the accuracy required.

Figure 1(a) shows the raw spectrum of the comet, averaged over all the reliable scans and corrected to the top of the atmosphere but before correction for the instrumental response, minus an average spectrum of the G stars normalized in the vicinity of 4500–5000 Å. Subtraction of a solar spectrum is often more effective in bringing out weak emission or absorption features than is division by a solar spectrum (see, e.g., Cochran *et al.* 1980). Differences in color between comet and Sun, multiplied by the response function of the spectrometer, appear as the overall depression below zero between 3100 and 3700 Å and as the overall excess above zero from 5500 to 7500 Å. As noted above, the region

TABLE III. Grain properties.

Date	r [AU]	ϕ^1 [deg]	ρ^2 [10^4 km]	$Af\rho^3$ [10^3 cm]	CE ⁴ [mag]
80/11/14.5	5.55	8.0	4.35	4.35 \pm 0.44	>1.6
81/1/5.4	5.25	10.7	5.11	(7.3 \pm 3.0)	.92
81/3/12.4	4.78	3.3	2.72	6.16 \pm 0.21	.42
81/4/5.4	4.64	2.3	5.12	6.85 \pm 0.15	.34
81/4/6.4	4.63	2.6	1.80	7.79 \pm 0.32	.25
82/1/30.5	3.39	14.0	3.89	4.73	-
82/3/6.5	3.36	16.9	4.60	4.21 \pm 0.06	.26
82/3/24.5	3.37	17.2	4.27	3.32 \pm 0.30	.20
82/3/26.3	3.37	17.2	5.63	3.50 \pm 0.14	.35
82/3/27.3	3.37	17.1	2.78	3.92 \pm 0.20	.31
82/3/28.3	3.37	17.1	2.01	3.78 \pm 0.14	.36
82/3/29.4	3.37	17.1	11.02	3.28 \pm 0.19	.34
82/3/30 -4/2	3.37	17.1	4.38	3.46 \pm 0.2	-
82/4/23.5	3.39	15.0	3.99	4.26 \pm 0.17	-
82/4/24.5	3.39	14.9	4.99	6.27 \pm 0.42	-
82/4/25.5	3.39	14.8	2.52	4.10 \pm 0.18	-
82/4/28.5	3.39	14.3	3.92	4.42 \pm 0.18	-
82/4/28.4	3.39	14.4	2.78	5.30 \pm 0.10	.16
82/4/30.4	3.40	14.0	0.95	4.79 \pm 0.15	(2.58)
			0.22	2.05 \pm 0.25	.26
			0.94	4.42 \pm 0.10	.92
82/5/29.4	3.45	7.7	1.78	5.47	.21
82/5/30.4	3.45	7.4	1.78	5.34 \pm 0.03	.34
82/6/24.3	3.51	0.2	1.77	7.76 \pm 0.03	.32

1. Phase angle = 180° - scattering angle
2. Radius of field of view.
3. Product of albedo at $\lambda 5240$, filling factor, and radius of field of view; see text.
4. Color excess = $(m_{3675} - m_{5240}) - 1^{m106}$ where 1^{m106} is observed color of solar analogs.

between 4000 and 4500 Å was not observed because it would have required rearranging the order-separating filters within the filter slide of the scanner.

The emission band of CN at 3883 Å is obvious. Not so obvious but definitely present is the $\Delta v = 0$ sequence of C₂ with head at 5165 Å. The presence of this band sequence of C₂ has not been reported for this comet by any of the spectroscopic observers but they, in general, do not have spectra with high signal-to-noise ratio of regions far from the nucleus. Also not so obvious in this raw spectrum because of the very low instrumental sensitivity is the emission by the 0-0 band of OH at 3085 Å. There is an additional feature present in the vicinity of 7200-7300 Å. Although it is obvious that the continuum has not been correctly subtracted in this region, it appears that a correct subtraction would leave an emission feature. Since the absolute count rates were much lower here than at the C₂ feature, we suspect that this feature is just noise, as are the weaker features between 4500 and 5000 Å, where count rates were down by a factor of 2.

Figure 1(b) shows the ratio of the cometary spectrum to the average G-type spectrum. The noise just shortward of the C₂ feature is considerably amplified in this figure, com-

pletely masking the presence of the C₂. The OH, which was visible but not strong in Fig. 1(a), is now clearly a strong feature. One can also see from this figure that the reflectivity of the comet increases slowly with wavelength and that there does appear to be some structure in the reflectivity curve at the shortest wavelengths. The net fluxes ($\text{erg cm}^{-2} \text{s}^{-1}$) in the emission bands are 5×10^{-13} for OH, 8×10^{-13} for CN, and 8×10^{-13} for C₂. Note that, although the CN feature seems much clearer than the C₂ feature, it actually contains no more flux because it is far sharper; it merely contrasts better with the continuum.

There are numerous sources of error in these data. In general the "sky" presumably included many stars just below the level of detection. The comet's motion at this time was approximately 30 arcsec/hr so that it moved over several different skyfields during the course of each night's observations and observations on different nights were in completely independent regions of the sky. The night-to-night fluctuations in net counts for each wavelength point were typically of order 10% and apparently completely random indicating that the subtraction of sky, which was typically near half of the total comet-plus-sky, left no systematic errors above a few percent. A potentially more serious problem is due to the

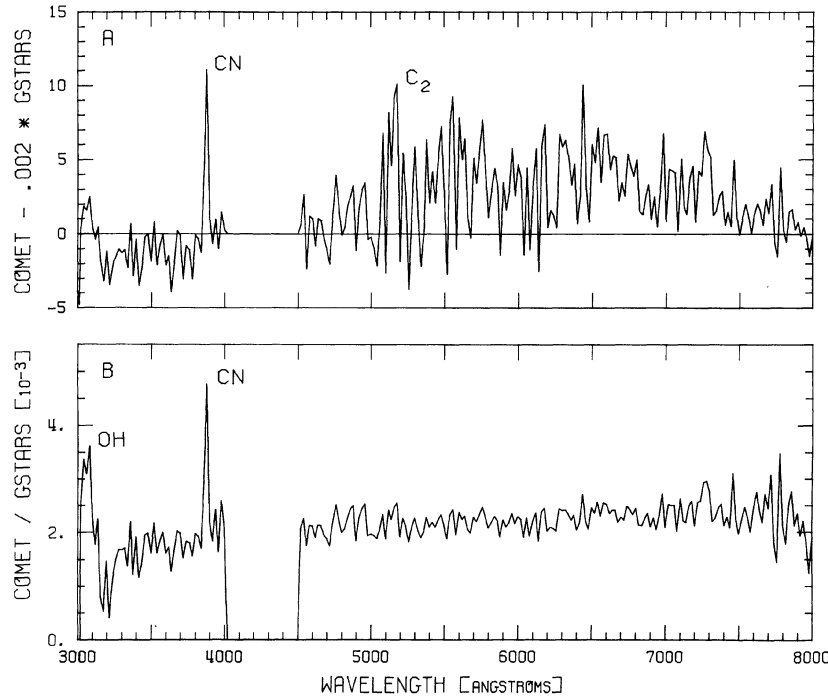


FIG. 1. (a) Raw, average spectrum of Comet Bowell after subtraction of normalized, average, raw spectrum of G stars. Use of raw spectrum before correction for instrumental response shows C_2 band at λ 5140 which gets masked by noise at shorter wavelengths when spectrum is divided by instrumental response function. Emission by CN is clear at λ 3883. Emission by OH is visible at λ 3085 Å. (b) Ratio of spectrum of Comet Bowell to average spectrum of G stars. This removal of the instrumental response masks the C_2 emission by enhancing noise at $\lambda < 5000$ Å but makes the OH emission clear. Data points shortward of λ 3060 deviate from unity by less than 1σ .

fact that the gaseous portions of the comet extend into the sky-subtraction aperture. This will cause us to systematically underestimate the flux in the emission bands. The effect will be larger for OH and C_2 than for CN because, as we will argue below, these two species likely came partly from a distributed source (the grains) in this particular comet. The fluxes for OH and C_2 are probably not much more accurate than a factor of 2 because they are extremely sensitive to assumptions about the amount of continuum to be removed. Nevertheless, we can use them to derive production rates and we find $\log Q$ values 28.04, 25.82, and 25.56 s^{-1} for OH, CN, and C_2 , respectively. These are in remarkably good agreement with the results from the filter photometry in the several days immediately preceding this observing period. We therefore have confidence that our detection of these emission features via filter photometry is real.

c) Ultraviolet Spectrophotometry

An ultraviolet spectrum of Comet Bowell was obtained with the Long Wavelength Spectrograph (LWR) of the IUE spacecraft on 27 April 1982 ($r = 3.393$, $\Delta = 2.744$ AU). The spectrum was exposed in segments, in order to periodically check the tracking of the spacecraft, over the interval 1115–1742 UT for a total exposure of 330 min (IUE image LWR 13088). The line-by-line spectra provided by the IUE project were processed with our own software to extract the spectrum for a 10.3×15.2 arcsec ($2.03 \times 3.02 \times 10^4$ km) area centered on the nucleus of the comet. This software allows optional median filtering of the spectrum as well as background, variable smoothing, and several comparisons with solar spectra. One resultant spectrum, based on the revised calibration of the sensitivity of the LWR camera (Holm *et al.* 1982) and smoothed with a hanning function, is shown in Fig. 2. The emission feature of OH is evident although it is

noisy, just as in the optical spectrum. Features longward of OH are due to noise which has been amplified in dividing by the rapidly decreasing response function.

As in the optical, the flux in an emission feature is very sensitive to the subtraction of the underlying continuum. Also shown in Fig. 2 is a normalized solar spectrum as deduced from IUE observations of solar analogs selected by Hardorp (1982, and references therein). These observations were taken by a number of different investigators and were obtained by us from the IUE archives, and the present spectrum is a preliminary one only. In this case the solar spectrum was normalized to the cometary spectrum for the spectral interval 3000–3050 Å and then subtracted from the cometary spectrum point by point to derive the OH emission. A variety of other reductions were used and yielded a total variation of $\sim 25\%$ in the flux of the OH emission. The resultant flux in the 0–0 band of OH is $8 \times 10^{-14} \text{ erg cm}^{-2} \text{ s}^{-1}$ which leads to a production rate of OH, $Q(\text{OH}) = 1.4 \times 10^{28} \text{ s}^{-1}$. This value of the production rate is consistent with the preceding and following determinations from filter photometry.

Additional IUE exposures, each of approximately 5.5-hr duration, were obtained by M. C. Festou from the European Control Center near Madrid, Spain on 22 and 28 May 1982. These exposures yield spectra very similar to that obtained on 27 April and have been processed in the same manner to derive additional OH production rates, which are given in Table II.

d) Combining the Continuum Data

The data on emission bands are readily comparable even though they may have been taken with different instruments and different fields of view because there are standard prescriptions for reducing the fluxes to production rates which

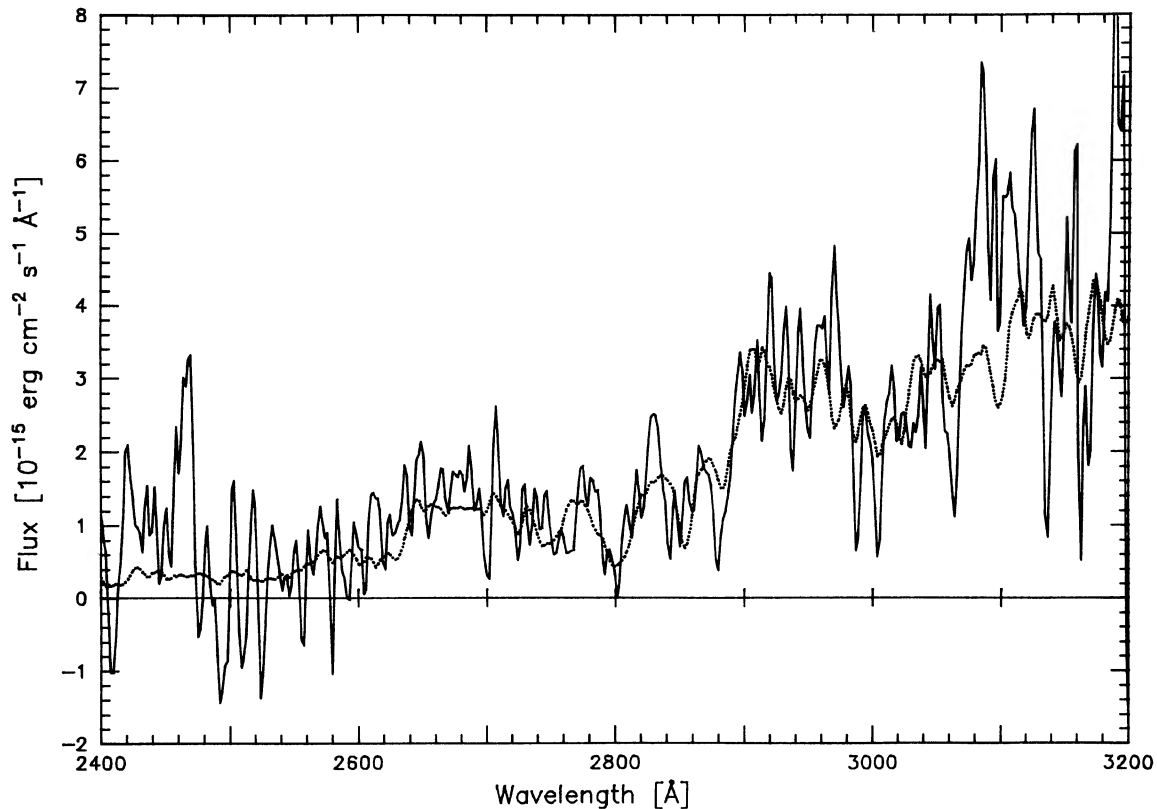


FIG. 2. IUE spectrum of Comet Bowell (solid line) and average IUE spectrum of solar analogs (dashed line) normalized for interval $\lambda\lambda$ 3000–3050 Å. Emission by OH is clear at 3085 Å. Features near both ends of the figure are due to noise in regions where signal was weak. Longward of OH, removal of instrumental response has enhanced the noise.

are then independent of the observational circumstances. Numerous publications have shown that the results, even if systematically in error, are at the very least internally consistent for most comets and the discussion above shows that the results are self-consistent for Comet Bowell. For the continuum data, however, there is no widely accepted procedure for combining various sources of data. As discussed in Sec. II, we have chosen to use the quantity Afp , which should be independent of aperture size on the radial outflow model, to combine data taken with apertures of different sizes, and we will use filter photometric data to relate spectrophotometric data taken at different times.

The use of the quantity Afp can be justified in part by the spatial profile of the brightness of Comet Bowell obtained by Jewitt *et al.* (1982). They found that the surface brightness followed a ρ^{-1} dependence out to $\rho = 5 \times 10^4$ km (in February 1981) as expected from a radial outflow model and showed a sharp cutoff beyond that point. Our data from 24 March–4 April 1982 have been combined in Fig. 3(a). The figure shows the value of Afp (at 5240 Å) deduced from filter photometry with five different diaphragms (spanning a full order of magnitude in size) and two different telescope-photometer-filter combinations as well as from the optical spectrophotometry. It is clear that Afp varies only slowly with aperture size; the least-squares fit of a straight line through the data deviates from horizontal by less than one standard deviation. We therefore conclude that observations with ap-

ertures of different sizes can be combined by reducing them to the quantity Afp , at least within the range of sizes considered here. Figure 3(b) also shows a comparison of the wavelength dependence of Afp (normalized at 5240 Å) as deduced from spectrophotometric data with that deduced from filter photometric data. Again the agreement is excellent. Although we do not have comparable data to allow such comparisons at other times, these comparisons are sufficient to show that the filter photometry is suitable for direct comparison with the spectrophotometric data and that in the spring of two different years (1981 and 1982) the surface brightness varied as ρ^{-1} over radial distances in the approximate range 10^4 – 10^5 km.

In order to study the reflectivity as a function of wavelength over the complete spectral range for which we have data, it is also necessary to allow for the fact that the spectrophotometric data were obtained over an interval of more than a month. Fortunately we have available filter photometric data contemporaneous both with the optical spectrophotometric data and with the IUE and infrared observations. Examination of Table II shows that the quantity Afp (at λ 5240 Å) increased significantly during April 1982. If we ignore the observation on 30 April with the 2.2-arcsec aperture, which was extremely sensitive to guiding errors, we find that the Afp values for the optical spectrophotometry should be increased by a factor 1.35 ± 0.02 in order to be combined with the IUE results. This increase could be due

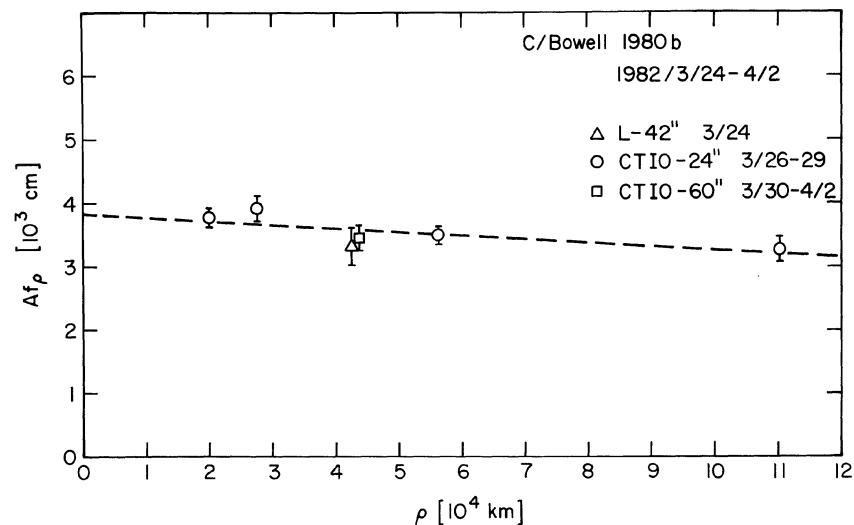


FIG. 3. (a) Variation of $Af\rho$ with radius of diaphragm, ρ . Combines data from both photometry and spectrophotometry. Straight line, fitted by least squares, deviates from horizontal by less than one standard deviation showing that $Af\rho$ is independent of aperture.

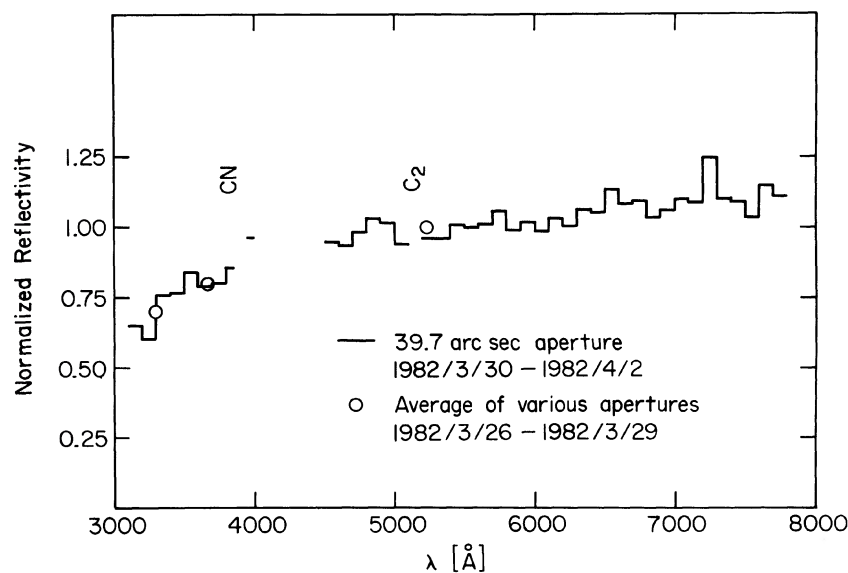


FIG. 3. (b) Variation of $Af\rho$ with wavelength. The open circles are based on filter photometry and show that the photometric data are equivalent to the spectrophotometric data for measuring colors. The short gaps in the spectrophotometric data correspond to points contaminated by emission bands of CN and C₂ as indicated.

either to activity by Comet Bowell during April 1982 or to a change in the scattering angle. As will be discussed below, both effects probably contribute.

III. CONTINUUM REFLECTIVITY AND ACTIVITY

Our ultraviolet spectrum was obtained at the same time as and with a similar field of view to that of both near-infrared photometry of the comet (A'Hearn *et al.* 1984; observations 23-26 April 1982) and the optical photometry in Table II. It is therefore totally appropriate to compare them directly. Figure 4 shows the value of $Af\rho$ deduced from the 10×15 -arcsec aperture of the IUE and from a 9.6-arcsec diaphragm in the infrared. It also shows the values deduced from the optical spectrophotometry with a 39.7-arcsec diaphragm corrected by the factor 1.35 mentioned above to allow for the fact that the comet brightened in the interval between the optical observations and the infrared and ultraviolet observations. It is clear that the optical data connect very well

with both the ultraviolet and the infrared data indicating again that the method of correction for temporal changes is valid.

The infrared magnitudes of A'Hearn *et al.* (1983) were reduced to absolute reflectivities using the calibration of the H mag by Beckwith *et al.* (1976), the solar flux at H of Labs and Neckel (1968), and the measured colors of the solar analogs. The optical and ultraviolet spectrophotometric fluxes were reduced from relative (based on the solar analogs) to absolute reflectivities using the solar fluxes of Neckel and Labs (1981) in the interval λ 5200-5300 Å and of Broadfoot (1972) in the interval λ 2700-2800 Å. These spectral regions were all chosen to be regions of high signal-to-noise ratio in the data for the solar analogs.

The shape of this reflectivity curve is surprising. It is significantly lower in the near ultraviolet than in the visible. (Strictly speaking, we are discussing the variations of $Af\rho$ with wavelength and both A , the albedo, and f , the filling factor which includes the extinction efficiency, can vary with

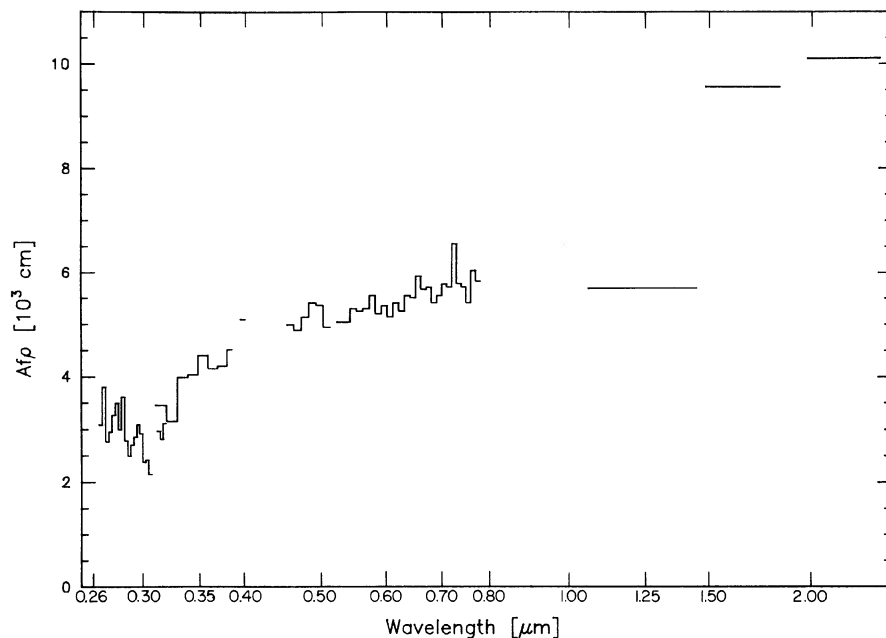


FIG. 4. Variation of albedo with wavelength. Ordinate is product of albedo, filling factor of diaphragm, and projected radius of diaphragm. IUE data (10×15 -arcsec aperture) are plotted from 2600 to 3165 Å, scaled CTIO spectrophotometric data (39.7-arcsec aperture) from 3100 Å to 8000 Å, and IRTF photometric data (9.6-arcsec aperture) at longer wavelengths. Decrease of albedo from λ 2600 to λ 3000 is marginally significant ($2-3\sigma$). Structure at longer wavelengths is highly significant.

wavelength. We will, however, assume that it is the albedo which is varying.) The decrease in albedo from 2600 to 3000 Å is marginally significant (about $2-3\sigma$, limited by the rather poor statistics of the data). The subsequent IUE spectra yield a uniform or slightly increasing ultraviolet albedo, suggesting that the decreasing albedo on 27 April was either spurious or associated with the onset of outburst (see below). The slight discrepancies between IUE and ground-based data in the range 3000–3200 Å are due to the fact that both signals were very weak in this region. There are no statistically significant absorption features or other spectral signatures which would indicate the presence of certain ices (e.g., SO_2) in the grains (Hapke *et al.* 1981). Features in the IUE spectrum (Fig. 2) other than that of OH do not repeat in the other spectra from IUE. The magnitude of the darkening in the ultraviolet relative to the visible is of the same order as that found by Feldman (1980) for Comet West (1976 VI), while the uniform albedo from 2600 to 3000 Å was seen in Comet West and in several other comets observed with IUE (Weaver *et al.* 1981).

The dramatic increase in Afp in the near infrared has not been reported for other comets. One might suspect several sources of error that could produce this discrepancy but they do not explain it away. The beam of the telescope used for the infrared photometry is somewhat vignetted but the field of view was directly measured by obtaining spatial scans across point sources and shows no wavelength dependence. (Omission of the correction for this vignetting would have led to much higher values of Afp at all infrared wavelengths.) Care was also taken to insure that field stars did not contaminate these measurements.

The measurements suggest very different behavior for smaller fields of view in both the optical and the infrared but the infrared field of view used here almost exactly matches that used for the optical photometry on 28 and 30 April and is only slightly smaller than the ultraviolet field of view. The infrared data of A'Hearn *et al.* (1983) show that in a smaller aperture (5.4 arcsec) Afp is nearly constant with wavelength

at 6×10^3 cm but the optical data with a 2-arcsec aperture show a very low value of $Afp = 2 \times 10^3$ cm. Although this latter result is very sensitive to guiding errors, and therefore not reliable, it suggests that the particles near the nucleus may be quite different from those further from the nucleus.

The combination of the differences in Afp near the nucleus, the significant increase in the optical Afp value between March and April, and the gas production to be discussed below, argues strongly for the presence of recently released grains in the coma in April of 1982. If Sekanina's (1982) model is correct in predicting very large grains in the old coma, then the present observations suggest that smaller grains have been recently released from the nucleus and have been swept out to the outer coma by the time of our 30 April 1982 observations. The darker material at the center is composed of the residual large grains which were essentially unaffected by the more recent outflow.

Figure 5 shows a different aspect of the reflectivity of the grains. We have plotted the quantity Afp for the wavelength 5240 Å as a function of phase angle, combining data from the several apparitions of Comet Bowell. Phase angle 0° (back-scattering) divides the pre-perihelion data from the post-perihelion data. The phase angle was not monotonic with time (heliocentric distance) during the pre-perihelion phase and arrows indicate the progression of time. For the post-perihelion data, the phase angle decreased monotonically with time. There are two effects seen in this figure, both a strong dependence of scattering efficiency on phase angle and also temporal changes in the comet. The data strongly suggest that, for a given phase angle, the comet was significantly brighter in the winter of 1981–1982 than in the winter of 1980–1981. This is presumably due to release of new grains which we see superimposed on the older grains. These new grains seem to contribute about one-fourth of the total scattered light at λ 5240 in 1981–1982. Another temporal change is suggested by the data in April of 1982, approximately one and one-half months after perihelion. These data suggest that a discrete outburst occurred in late April 1982. The data

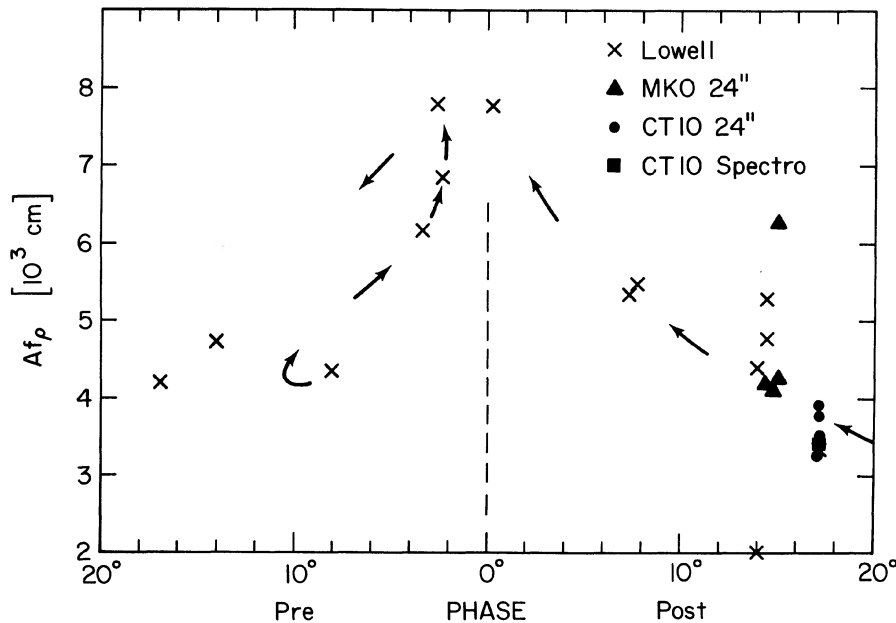


FIG. 5. Phase variation of albedo at λ 5240 as given by the parameter Af_p . Pre-perihelion data are to the left of phase = 0° (scattering angle = 180°) with arrows indicating progression of time. Apparently there were some "new" particles present by April 1981. The post-perihelion data, to the right of phase = 0° , are monotonic with time as indicated by the arrows. We infer that the backscattering peak is roughly $3\times$ higher than the scattering at moderate phases.

from Mauna Kea are rather unreliable because of the very patchy atmospheric extinction produced by the dust from the eruption of El Chichon but the observations from Lowell Observatory should not be affected by this. (The dust did not affect observations that far north until much later in the year, by which time the dust was much more uniform.) Short-term fluctuations such as this have also been reported in the infrared by Campins (private communication).

Despite these temporal changes, the effect of phase angle clearly stands out above the uncertainties due to the temporal changes. It appears that the backscattering peak is approximately a factor of 3 higher than the scattering would be at moderate phase angles in the range 30° – 90° where the scattering is likely to be independent of phase angle (e.g., Ney and Merrill 1976). This peak is significantly higher than found by Dobrovolskij *et al.* (1979) for Comet Ashbrook-Jackson 1977g and by Millis *et al.* (1982) for Comet P/Stephan-Oterma 1980g. This would be expected if the "new" particles were typical cometary particles superimposed on old, large particles with a much stronger backscattering peak.

Examination of the color excesses in Table III also suggests changes in color both with phase angle and with activity. The observations prior to April 1981 yield significantly redder colors than are typical after that time. This suggests that the "old" particles are very red and the newer ones less red, perhaps because the newer ones are much smaller. The anomalously red colors recur in April of 1982 when several pieces of evidence indicate transient activity. These temporal fluctuations mask the phase dependence of the color. There is a suggestion in the post-perihelion data that the color is slightly redder away from the backscattering region but the uncertainties in the data are too large to conclude that the effect is real.

IV. GAS PRODUCTION

Figure 6 shows the production of OH and CN, taken from Table II, as a function of time. The most striking thing about

this figure is the fact that the production of OH (but not that of CN) peaked nearly a year before perihelion at a heliocentric distance near 4.5 AU. Although there are no spectroscopic confirmations of the presence of emission from OH at this time, spectra by Larson (private communication) and spectral scans by Cochran (private communication) do not have sufficient sensitivity to show even the continuum of Comet Bowell in this spectral range. The subsequent agreement between filter photometry and spectrophotometry in 1982 gives us confidence in the results. With our photometric technique, the comet was readily detectable in all filters in the ultraviolet. The limit to our accuracy was set primarily by the uncertainty in the fraction of the signal that was due to continuum.

After this peak, the production of OH decreased by nearly a factor of 10 in the interval from April 1981 to January 1982. There was then a major outburst roughly one month after perihelion. Our interpretation of this phenomenon, discussed further below, is that the OH production at $r_H = 4.5$ AU was due primarily to vaporization of H_2O from the old grains. By the time perihelion was reached, all H_2O had vaporized from the old grains but it was then being produced from the nucleus directly and/or from new grains being dragged out from the nucleus at that time. The post-perihelion outburst presumably originated in the nucleus but the production of OH continued for some time because of continued vaporization of the icy grains released during that outburst.

An examination of Table II and Fig. 6 shows that CN, widely observed spectroscopically in 1982, was being produced then at a rate of somewhat less than 1% that of OH, a value which is somewhat high but in the range observed for other comets in our program. Our earlier observations of CN consist of only one positive detection plus several upper limits. All of these data imply that CN production was anomalously low relative to that of OH in 1980–1981. This is easily understood if the parent of CN is highly volatile and can diffuse out of the grains in the several years between their

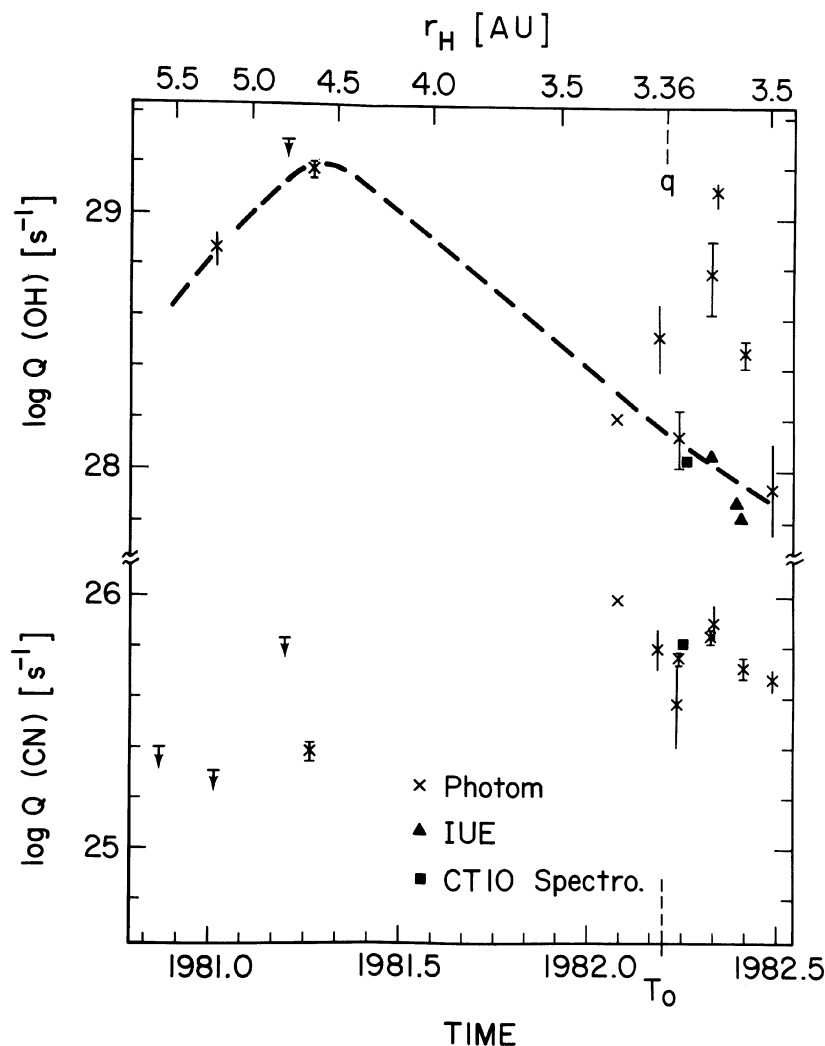


FIG. 6. Production of OH and CN vs time. Dashed line (drawn free hand) suggests the quasi-equilibrium behavior for OH. Error bars shown as | are based on comparison of independent observations with different fields of view as in Table II. Error bars shown as \perp are based purely on the photometric precision of Table I and are presumably lower limits. Errors for spectrophotometric results (\blacksquare and \blacktriangle) are estimated at 25%–50% (i.e., ± 0.1 – 0.3 in $\log Q$). Note that the error bar is very small for the point near the peak of the OH curve in spring 1981. It appears that the OH production peaked in spring 1981 and then declined. The CN was undetectable in the early stages and clearly did not exhibit anomalously high production in spring 1981 when the production of OH was very high.

release from the nucleus and the onset of vaporization of H_2O or if the parent of CN (presumably HCN) was primarily in the more volatile matrix binding the grains of H_2O . The normal proportion of OH seen subsequently is due to vaporization of material that was in the nucleus and from which the CN parent could not diffuse. Similarly, the CN was less abundant relative to OH during the outbursts, a fact which can also be understood if the outburst originated in mid-to-late April and released the CN parent directly together with many icy grains. These grains would then continue to release H_2O by vaporization over a time scale of weeks.

The C_2 radical is much harder to detect than is CN because its emission features have much lower contrast with the continuum. Nevertheless, during 1982 we consistently detected C_2 , albeit with rather large uncertainties in some cases, and these fluxes imply production rates somewhat greater than those of CN, in qualitative agreement with our findings for most other comets. The C_3 radical was generally not detectable although the upper limits on the production of C_3 are not significantly lower (relative to C_2 or CN) than observed production rates in other comets.

We find, therefore, that the relative chemical abundances in the coma of Comet Bowell were probably normal during

quasi-equilibrium behavior near and after perihelion. Well before perihelion and during the post-perihelion outburst, however, OH was significantly overabundant compared to other species.

V. A MODEL

Our hypothesis regarding the production of OH from old grains in the spring of 1981 can be checked quantitatively. The peak production rate of OH was found to be somewhat less than $2 \times 10^{29} \text{ s}^{-1}$ but this number is based, for consistency with our other photometric results, on the standard parameters of the Haser model used in the data reduction including a lifetime of $1.16 \times 10^5 \text{ s}$ at 1 AU. As pointed out by Festou (1981), the Haser model systematically underestimates the true lifetime of the species being observed. Furthermore, Jackson (1980) has shown that the lifetime of OH is sensitive to its heliocentric velocity. Singh *et al.* (1983) and Schleicher (unpublished) have recalculated the dissociation lifetime of OH using the methods of Jackson. Schleicher finds that the lifetime for the relevant heliocentric velocity ($\approx 10.5 \text{ km/s}$) should be approximately $2.4 \times 10^5 \text{ s}$ at 1 AU but van Dishoeck and Dalgarno (private communication)

taking into account more dissociation channels, find a value near 2/3 this. This implies that the true production rate for April 1981 should be roughly 1/2 to 3/4 that given in Table II and in Fig. 6, i.e., $(8-12) \times 10^{28} \text{ s}^{-1}$. We now ask how much surface area must be in the grains to produce this vaporization.

Assuming that the grains are large ($\geq 0.5 \text{ mm}$), it is valid to consider them as bulk ice undergoing equilibrium vaporization, but because they are not very large we assume they are isothermal. We also assume that they are reasonably dark. Under these assumptions, the vaporization rate per unit area varies steeply with heliocentric distance and depends only on the difference between the visual and infrared albedos, not on the albedos themselves. As an example, the case of $A_{\text{IR}} = A_{\text{vis}}$ (at least for $A \leq 0.15$) yields a vaporization of $6 \times 10^{10} \text{ cm}^{-2} \text{ s}^{-1}$ at a temperature of 130 K which is the blackbody temperature for $r_{\text{H}} = 4.6 \text{ AU}$. Changing the albedo difference to ± 0.10 would change the vaporization by roughly a factor of 4 in either direction and the temperature by roughly $\pm 4 \text{ K}$ without changing the variation with r_{H} . Since the vaporization rate can vary by an order of magnitude for such small changes in albedo, it is essential to consider other information. During April 1981, the same month in which we observed the peak production of OH, Jewitt *et al.* (1982) deduced a temperature of $140 \pm 10 \text{ K}$ from broadband photometry of the thermal infrared radiation. Independent of any assumptions about albedo, this temperature corresponds to a vaporization rate of $1.5 \times 10^{12} \text{ cm}^{-2} \text{ s}^{-1}$. Although temperatures above the black body temperature are usually associated with small particles (which have low effective albedo in the infrared), they can be produced entirely by differences between the infrared and visual albedo even in large particles. For the purposes of calculation, we will assume that the effective vaporization rate was near the middle of the range cited above, $5 \times 10^{11} \text{ cm}^{-2} \text{ s}^{-1}$ in Comet Bowell at 4.6-AU preperihelion. The observed production rate of OH at this time thus requires an effective, vaporizing surface area of $1.6 \times 10^{17} \text{ cm}^2$. Note that if this surface area were on an isothermal, spherical nucleus, the radius would exceed 1000 km, orders of magnitude larger than estimated for any other comet.

If the cometary grains were spherical, their total cross section would be just one-fourth their surface area or $4 \times 10^{16} \text{ cm}^2$. Since the grains are more likely irregular and fluffy, their cross section might be substantially less than this value but at present we have no way of estimating the degree of fluffiness, so we will assume for the purposes of calculation that the particles are spherical. In April of 1981 the product of Afp was observed to be roughly $7 \times 10^3 \text{ cm}$ in apertures with ρ up to $5 \times 10^4 \text{ km}$. According to Jewitt *et al.* (1982) this radius corresponded to the sharp outer edge of the coma of Comet Bowell. We therefore estimate the total grain albedo \times cross-section product for comet Bowell at $N\alpha A = Afp\rho_{\text{max}}^2 = 10^{14} \text{ cm}^2$. If the total cross section, $N\sigma$ has the maximum value deduced above on the assumption of spherical particles, we find that the albedo of the particles near backscattering is 0.0025. Recall that our definition of albedo is such that if the scattering were isotropic, this albedo would represent the fraction of incident light which is reflected, a definition which is greater than $A_p(\theta)$ defined by Hanner *et al.* (1981) by a factor four times the scattering efficiency.

If the particles are fluffy such that the ratio of cross section to total surface area is a few times lower than its maximum

for spherical particles, the albedo is correspondingly a factor of a few higher, i.e., about 1%. In either case the albedo is remarkably low, much lower than the values estimated by infrared observers from the ratio of thermal to reflected flux. It is orders of magnitude higher than the albedo implied by the occultation result reported by Combes *et al.* (1982), a result which seems questionable on several grounds (cf. Combes *et al.* 1983). Interestingly another reported occultation by Comet Bowell (Larson and A'Hearn, in preparation) implies a visual albedo (per our definition) near 0.002, in close agreement with the results of our approach. Note also that if the particles are fluffy the effective albedo will be substantially less than the albedo of bulk material because of multiple reflections. In fact, if a typical photon scatters twice before emerging, the effective albedo will be just the square of the albedo of the bulk material.

Continuing with our nominal calculation for spherical particles, we can also estimate the total number and mass of grains in the coma if we assume that the typical grain radius is 1.0 mm, consistent with the results of Sekanina (1982). If we assume a density of 1 g cm^{-3} , then the total number of grains is 10^{18} and the total mass is $5 \times 10^{15} \text{ g}$ (corresponding to $\sim 1 \text{ m}$ on a 10-km nucleus). This substantially exceeds Sekanina's lower limit of 10^{13} g but that was based on an assumed albedo two orders of magnitude higher than deduced in our calculations. As noted above, our estimate is probably an upper limit since the most obvious complication, irregular particles, increases the albedo and thus decreases the cross section and mass. We conclude that production of the observed OH in April of 1981 is possible by our hypothesis of vaporization of water from the pre-existing large grains proposed by Sekanina.

It remains to consider the lifetime of the grains and explain the OH production observed in 1982. As the comet approaches the Sun, the vaporization rate from the grains increases rapidly and by January 1982 ($r = 3.4 \text{ AU}$) the vaporization rate deduced for 4.6 AU should have increased by a factor of order 500. An average vaporization rate over those eight months then would have been of order $10^{14} \text{ cm}^{-2} \text{ s}^{-1}$ which corresponds to roughly 1 mm of ice per year. It seems clear, then, that all the original ice should have disappeared from the grains by the time the comet approached perihelion. The source of the OH observed near perihelion, then, must be the activity of the nucleus itself. As originally pointed out by H. U. Keller (1983), the calculations by Cowan and A'Hearn (1979) show that vaporization from a nonrotating nucleus (or equivalently one with its rotation axis pointing toward the Sun) is much greater than from an isothermal body and can easily explain the observed production of OH. If we assume that both visual and infrared albedo are very low, as found above for the grains, we find that at perihelion the effective average vaporization rate from a nonrotating nucleus is $2 \times 10^{16} \text{ cm}^{-2} \text{ s}^{-1}$, while the observed production rate, before the outburst of April 1982, was somewhat less than 10^{28} s^{-1} (after correction of the lifetime of OH) implying a nuclear radius near 2 km. Even the much higher production during the outburst of April 1982 would require a nuclear radius less than 10 km, values which would be quite compatible with our current understanding of comets. At the time of the post-perihelion outburst, equilibrium vaporization of large, isothermal grains would yield $10^{14} \text{ cm}^{-2} \text{ s}^{-1}$, while the elevated temperature observed in 1981 would scale so as to yield $8 \times 10^{14} \text{ cm}^{-2} \text{ s}^{-1}$ and thus a lifetime of millimeter-sized grains of order months and cor-

respondingly smaller lifetimes for smaller grains. Thus our model is quantitatively realistic for producing the initial OH from grains and the subsequent OH from the nucleus. Furthermore, we suggest that in this regard Comet Bowell was typical of dynamically new comets as also suggested by Sekanina (1982).

VI. SUMMARY

Observationally we find that Comet Bowell began to produce significant amounts of OH (but not other species) long before perihelion at a heliocentric distance near 4.6 AU. This production then decreased as the comet approached perihelion at 3.4 AU and other species such as CN and C₂ appeared with their normal abundances. An outburst in April 1982 was dominated by OH. We also find that the grains in 1982 (near perihelion) exhibited significant increases in albedo between 3150 Å and 4500 Å and also between 1.2 μ and 1.6 μ. There was also significant transient activity, presumably due to outbursts, during 1982.

The data suggest the presence of two populations of grains, a very old population previously modeled by Sekanina (1982) which consists of very large (millimeter size), very red, very dark icy grains with strong backscattering and a recently released population of smaller grains which are much less red and more typical of grains in comets near the Sun. The ice on or in the large grains had totally vaporized by the time of perihelion, by which time the nuclear vaporization was producing measurable amounts of all the usual cometary species. The effective visual albedo of the grains is

probably of order 1%, much darker than estimated by other techniques. The nucleus of Comet Bowell is probably larger than most cometary nuclei, but still not more than 10 km in radius, and the activity at very large distances which released the old population of large grains must have removed at least several meters of ice from the surface.

We concur with Sekanina's (1982) suggestion that Comet Bowell was physically, if not dynamically, a very typical new comet entering the inner solar system from the Oort cloud for the first time.

We thank the staffs of the various observatories involved in this program for their cooperation in attempting to coordinate the numerous observations as well as for their assistance during the observations. Archival data from IUE were provided by the National Space Science Data Center. S. Larson and A. Cochran kindly provided much spectroscopic and spectrophotometric information. We had helpful discussions with numerous people including H. Campins, M. Festou, D. Jewitt, M. Hanner, and H. U. Keller. The ground-based observing was supported by NASA Grants NSG 7322 to the University of Maryland and NGR-03-003-001 to Lowell Observatory. The observing with IUE was supported by NASA Grants NAG 5-252 to the University of Maryland and NSG 5393 to the Johns Hopkins University. Computing facilities were provided by the University of Maryland Computer Science Center.

REFERENCES

- A'Hearn, M. F. (1982). In *Comets*, edited by L. Wilkening (University of Arizona Press, Tucson), p. 433.
- A'Hearn, M. F. (1983). In *Solar System Photometry*, edited by R. Genet (Willmon Bell, Virginia).
- A'Hearn, M. F., Dwek, E., and Tokunaga, A. T. (1984). Submitted to *Astrophys. J.* (in press).
- Bowell, E. L. G. (1980). *IAU Circ.* No. 3461.
- Campins, H., Rieke, G. H., and Lebofsky, M. J. (1982). *Icarus* **51**, 461.
- Cochran, A. L., Barker, E. S., and Cochran, W. D. (1980). *Astron. J.* **85**, 474.
- Cochran, Anita L., and McCall, M. L. (1980). *Publ. Astron. Soc. Pac.* **92**, 854.
- Combes, M., Lecacheux, J., Sicardy, G., Zeau, Y., Encrenaz, T., and Vapillon, L. (1982). *IAU Circ.* No. 3751.
- Combes, M., Lecacheux, J., Encrenaz, T., Sicardy, B., Zeau, Y., and Malaise, D. (1983). *Icarus* **56**, 229.
- Dobrovolskij, O. V., Kiselev, N. N., Chernova, G. P., and Tupieva, F. A. (1979). In *Solid Particles in the Solar System*, IAU Symposium No. 90, edited by I. Halliday and B. A. McIntosh (Reidel, Dordrecht), p. 259.
- Everhart, E., and Marsden, B. G. (1983). *Astron. J.* **88**, 135.
- Feldman, P. D. (1980). In *Solid Particles in the Solar System*, IAU Symposium No. 90, edited by I. Halliday and B. A. McIntosh (Reidel, Dordrecht), p. 263.
- Festou, M. C. (1981). *Astron. Astrophys.* **96**, 52.
- Hanner, M. S., Giese, R. H., Weiss, K., and Zerrull, R. (1981). *Astron. Astrophys.* **104**, 42.
- Hapke, B., Wells, E., and Wagner, J. (1981). *Icarus* **47**, 361.
- Hardorp, J. (1982). *Astron. Astrophys.* **105**, 120.
- Holm, A., Bohlin R. C., Cassatella, A., Ponz, D. P., and Schiffer, F. A. (1982). *Astron. Astrophys.* **112**, 341.
- Jewitt, D. C., Soifer, B. T., Neugebauer, G., Matthews, K., and Danielson, G. E. (1982). *Astron. J.* **87**, 1854.
- Keller, H. U. (1983). In *Cometary Exploration*, edited by T. I. Gombosi (Hungarian Academy of Science, Budapest), Vol. 1, p. 119.
- Millis, R. L., A'Hearn, M. F., and Thompson, D. T. (1982). *Astron. J.* **87**, 1310.
- Neckel, H., and Labs, D. (1981). *Sol. Phys.* **74**, 231.
- Ney, E. P., and Merrill, K. M. (1976). *Science* **194**, 1051.
- Sekanina, Z. (1982). *Astron. J.* **87**, 161.
- Singh, P. D., van Dishoeck, E., and Dalgarno, A. (1983). *Icarus* **56**, 184.
- Weaver, H. A., Feldman, P. D., Festou, M. C., A'Hearn, M. F., and Keller, H. U. (1981). *Icarus* **47**, 341.